



Simulation of fouling in membrane processes with cellular automata

by A.M. Engelbrecht*, B. Bredenkamp*, and C. Aldrich*

Paper written on project work carried out in partial fulfilment of B Eng. (Chemical)

Synopsis

Membrane processes are vital to a diverse range of technical and biological systems, which also feature in mineral processing applications such as the treatment of mine effluent and extraction of metals. In this study, the use of cellular automata to model a semi-permeable membrane that separates two compartments is considered. Cellular automata are simple models that enable the analyst to represent well-understood local effects, such as the chemical or steric interaction between molecules themselves and between molecules or particles and their environment, which can lead to very complex behaviour on a macroscopic scale. Various physical phenomena, including reverse osmosis, were simulated. Initial results for the effect of temperature, membrane structure and chemical properties of the solutes on the performance of the membrane appear promising.

Keywords: cellular automata, dynamic modelling, filtration, membrane fouling, osmosis.

Introduction

An understanding of the movement of water and solutes across membranes is important in many technical processes, including a large variety of membrane filtration systems for the treatment of mine effluents and related wastewaters (Beneš *et al.*, 1983; Nenov *et al.*, 2006) and a range of hydrometallurgical processes (Flett, 1992; Sabba and Akretche, 2006). Transport processes through membranes are dynamic and depend on the membrane structure (porosity), as well as the chemical state of the membrane and the materials being transported.

In filtration where porous membranes are used, the most important disadvantage is the reduced permeate flux owing to fouling of the membranes (Dekker and Boom, 1995). Fouling is caused by pore plugging and adsorption of rejected macromolecules or other solutes in the membrane system. This requires periodic cleaning of membranes, which can add considerably to the overall cost of plant operation owing to lost productivity related to down-time, the cost of the chemicals used in cleaning, higher pressures and associated

pumping costs to maintain membrane productivity, as well as reduced lifetime of the membranes.

Although considerable progress has been made to overcome fouling, most of the proposed solutions cannot be implemented satisfactorily in practical membranes (Cui and Wright, 1994). The problem is compounded by the complex nature of fouling that is not fully understood as yet. As a result, models of fouling behaviour are often based on assumptions that may not represent the full spectrum of dynamic behaviour for membrane systems and more work is required to gain a better understanding of these processes. In this project, modelling of membrane phenomena, and fouling in particular, was explored by means of cellular automata, which allow the engineer to explore the effect of local phenomena on the overall behaviour of membrane systems, as will be explained in more detail below.

Cellular automata

Cellular automata are simple models that were introduced by Von Neumann (1966) and Ulam during the 1940s to study complex systems, such as biological processes (Sipper, 2002). A cellular automaton typically consists of a number of sites or cells arranged on a line or a regular lattice. The cells may take on any discrete values or states that evolve deterministically with time, based on a set of well-defined rules involving the values of the cells' nearest neighbours, as indicated in Figure 1.

* Department of Process Engineering, University of Stellenbosch, Stellenbosch, South Africa.

© The Southern African Institute of Mining and Metallurgy, 2007. SA ISSN 0038-223X/3.00 + 0.00. Paper received Mar. 2007; revised paper received Apr. 2007.

Simulation of fouling in membrane processes with cellular automata

Any system with identical discrete elements undergoing deterministic local interactions may be modelled as a cellular automaton. Physical examples include aggregation phenomena, such as the growth of snowflakes, growth of organisms into complicated forms through repeated application of simple local rules, and even the computer Game of Life (De la Torre and Martín, 1997).

Cellular automata are parallel processing computers in which the initial configuration encodes the program and input data, and time evolution yields the final output. According to Church's thesis in the formal theory of computation, such cellular automata can potentially simulate any possible system, examples of which are discussed by Vichniac (1984), among others.

Membrane model

In the case study, fouling in a reverse osmosis membrane used in a desalination process was considered. Based on the work done by Kier and Cheng (1997), the membrane system is modelled by using a lattice of squares, like that of a chess board. Each square or cell is designated to contain a particular substance or to be empty. Each cell is also confined by a Moore neighbourhood, as shown in Figure 1(b). Substances can move to adjacent cells, if these are empty or remain where they are, based on a given set of probabilities. The movement of all the cells is then computed for a given iteration or time interval. Figure 2 shows the set-up of the membrane system at the start of an experiment simulating the filtration of an aqueous salt solution with reverse osmosis.

The thin non-polar membrane initially separates two compartments of water. The flow of water into and out of the membrane is modelled, as well as the passage of solute through the membrane. Variation of the polarity of these solute cells gives an indication of the influence of this property on the behaviour of the system, as certain behavioural patterns emerge after a large number of iterations. In Figure 2, the model consists of a 100 × 100 grid of cells. The cells can assume any of five states, i.e. they can be empty (black), they can be membrane cells (pink) or contain water (turquoise), cations (yellow) or anions (purple).

The rules of the original model were based on the probability of adjacent cells i and j breaking apart (parting probability), $P_B(ij)$, as well as the probability of two cells joining up (joining probability), $P_J(ij)$ —values which depend on the state of the cells i and j . For example, pairs of substances showing a high affinity or interaction were simulated with high values of $P_B(ij)$ coupled with low values of $P_J(ij)$. Conversely, low values of $P_B(ij)$ coupled with high values of $P_J(ij)$ gave rise to model with dissimilar, non-interactive, repellent cell contents. For the new model used in the computerized simulations, the joining and parting probabilities are combined into a single interaction parameter, the swapping probability. The swapping probability represents the tendency of a cell to break apart from its existing neighbours and to swap with one of them, thereby joining a new neighbourhood.

Selection of interaction parameters for the membrane model

Through careful selection of the interaction parameters, the model can realistically accommodate changes in temperature, various degrees of solubility, the diffusion of solutes through a solvent, the effect of external directional forces, as well as other effects.

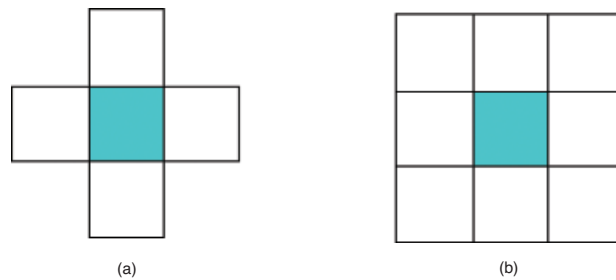


Figure 1—Neighbourhoods in two-dimensional cellular automata lattices: (a) Von Neuman neighbourhood (central cell in turquoise and N, S, E and W neighbouring cells) and (b) Moore neighbourhood (central cell in turquoise and N, S, E, W, NE, NW, SE and SW neighbouring cells)

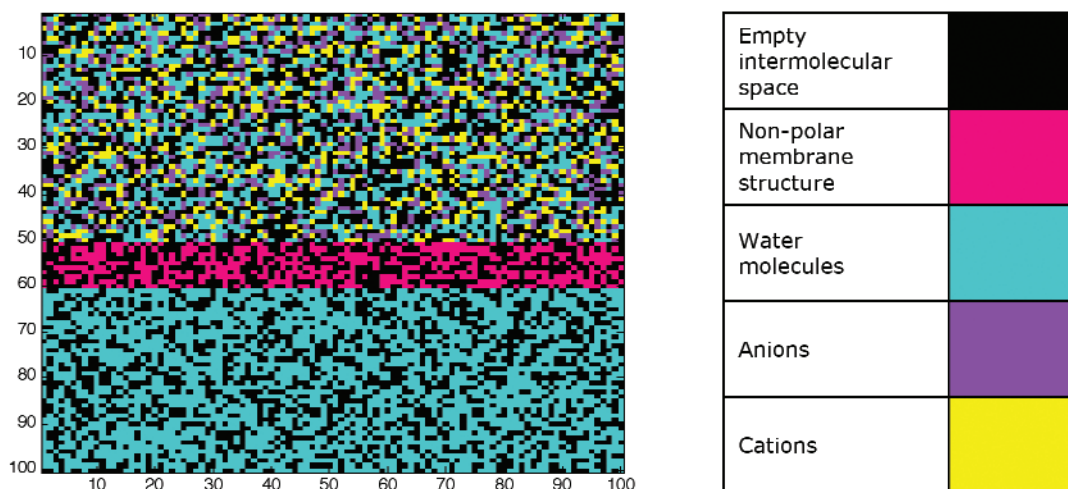


Figure 2—Start of a simulation with a cellular automata model of water compartments with membrane cells shown as a horizontal band in the centre

Simulation of fouling in membrane processes with cellular automata

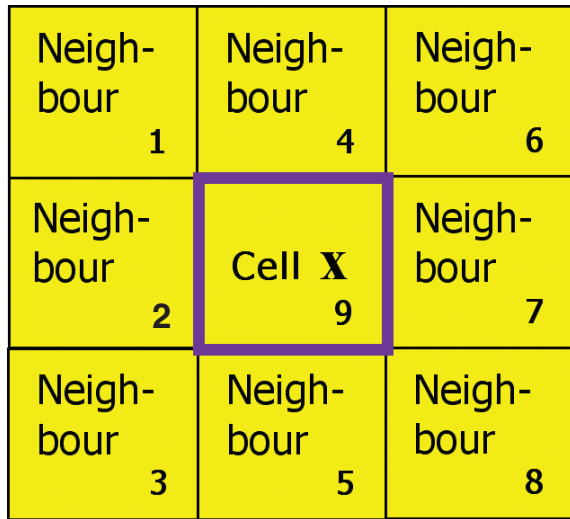


Figure 3—Indexed Moore neighbourhood (yellow) for Cell x (purple border)

The vector \bar{V} determines the directional bias for the movement of any cell within the 100×100 grid. The numbers in the bottom right-hand corner of each cell in Figure 3 depicts the sequence in which the neighbourhood cells appear in the vector (\bar{V}), including the cell for which the neighbourhood is considered (cell x).

Directional bias (cell movement owing to external directional forces)

For example \bar{V} is defined as follows: $\bar{V} = [3, 1, 1, 3, 1, 3, 1, 1, 1]$. For this definition the centre cell (x) will be three times more likely to move into position 1, 4 or 6 than any of the other surrounding positions. Therefore \bar{V} creates a predefined bias in the northern direction for this example. Note that the cell's current position (centre position = 9) also counts as one of the 'other positions' and that it is included the vector. Therefore the probability for the cell remaining in the same position has been accounted for.

This type of bias can be used to simulate the effect of an induced pressure drop, e.g. by means of a pump or an inclined flow duct. The directional bias therefore represents the effect of any external force on the osmotic system, which typically comes into play during reverse osmosis.

State bias (cell movement owing to internal osmotic effects)

The movement caused by the water potential difference within the osmotic system itself is modelled by means of a matrix, called the state bias. In order to construct the state bias matrix, the swapping probability of a cell has to be defined first.

The swapping probability (β_y), also called the score, is a scalar value that defines the probability for a neighbour (cell y), of the centre cell (cell x), which is surrounded by a specific combination of neighbours, to swap with cell x . Cell y is defined according to its position relative to cell x within the Moore neighbourhood. Therefore y is located in position 1, 2, 3, 4, 5, 6, 7 or 8 as defined in Figure 3. A weight (α) is attributed to each neighbour of cell y , depending on the state

of that neighbour. For example, if position 8 is considered as cell y , the Moore neighbourhood of cell y is shown in Figure 4 by position i up to ix (indicated in the top right-hand corner of the applicable cells). The swapping probability for cell y is defined in terms of α as follows:

$$\beta_y = \alpha_i \alpha_{ii} \alpha_{iii} \alpha_{iv} \alpha_v \alpha_{vi} \alpha_{vii} \alpha_{viii} \quad [1]$$

The neighbour (cell y = position 1, 2, 3, 4, 5, 6, 7 or 8) with the highest score (β_y) will exchange positions (swap) with cell x .

The state bias matrix ($\bar{\Omega}$) is a collection of possible weights from which every α is selected according to the state of the neighbour involved. The matrix is defined as follows,

$$\bar{\Omega}_y = \begin{bmatrix} a_{1,1} & a_{1,2} & a_{1,3} & a_{1,4} & a_{1,5} \\ a_{2,1} & a_{2,2} & a_{2,3} & a_{2,4} & a_{2,5} \\ a_{3,1} & a_{3,2} & a_{3,3} & a_{3,4} & a_{3,5} \\ a_{4,1} & a_{4,2} & a_{4,3} & a_{4,4} & a_{4,5} \\ a_{5,1} & a_{5,2} & a_{5,3} & a_{5,4} & a_{5,5} \end{bmatrix} \quad [2]$$

where $\alpha_{n,m}$ represents the weight with

n = state of cell y

m = state of the neighbour of cell y

For example if cell y (Position 8) represents water (state 3), with position i representing a void cell (state 1), then

$$\alpha_{\text{position } i} = \alpha_{3,1} \quad [3]$$

Trial runs were done in order to fine-tune the value of each $\alpha_{i,j}$ for a feasible model.

Model implementation

Selection of a directional and state bias

For a realistic model of an osmotic system, the state bias must be strong enough for the water molecules in the lower compartment to spontaneously move via the membrane

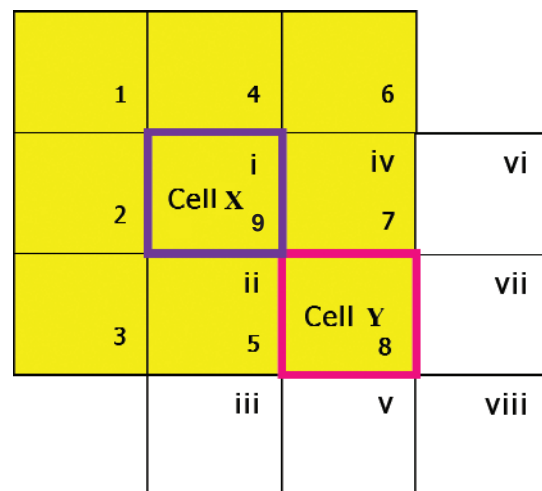


Figure 4—Indexed Moore neighbourhoods (yellow) for cell x (purple border) with cell Y (pink border) in position 8

Simulation of fouling in membrane processes with cellular automata

towards the upper compartment containing the salt ions, even for a neutral directional bias within the compartments. An iterative procedure was used to find a state bias.

The directional bias for the two compartments was chosen as follows:

$$\bar{V}_{\text{Compartments}} = [1, 1, 1, 1, 1, 1, 1, 1, 1] \quad [4]$$

For the membrane:

$$\bar{V}_{\text{Membrane}} = [0, 1, 0, 0, 0, 0, 1, 0, 0] \quad [5]$$

The directional bias for the two compartments represents a system with no flow in any direction except for the cell movements induced by the state bias (osmosis). The directional bias for the membrane ensures that the membrane cells move only in a horizontal direction. Therefore the membrane maintains its integrity and does not diffuse into the compartments during an experimental run.

The first iteration for a state bias was selected according to the following principles:

- ▶ Cells of certain states will have a great affinity for a neighbour of another state. These cells will have an inherent reluctance to exchange positions with an empty cell, which would cause them to separate from these neighbours.
- ▶ On the other hand, certain cell types also repel one another. If a cell is repelled by its neighbour, it will have a higher likelihood of swapping positions with an empty cell, possibly moving to a more favourable neighbourhood. If the next neighbourhood turns out to be unfavourable, the average swapping probability or mobility (β_y) of the cell with respect to its neighbours

will remain relatively high until it reaches a favourable neighbourhood. The β_y values will now decrease due to the increased affinity for its neighbours.

One of the key issues that had to be resolved in the model concerns the quantification, evaluation and comparison of the affinity of one cell type for another. Intermolecular forces provide the key to a feasible solution: by classifying each possible combination of states according to the strength and direction of their intermolecular interactions, the repulsion and resulting α value within each possible cell type combination can be evaluated and compared to that of another combination.

The mathematical dependency of β on α is summarized by the following relationships:

For an increasing β value: $\alpha_{ij} > 1$

For a decreasing β value: $\alpha_{ij} < 1$

For an unaffected β value: $\alpha_{ij} \sim 1$

These relationships dictate that for repulsion between cell x and y (if they represented type i and j respectively), $\alpha_{ij} > 1$, for a high affinity of type i for type j , $\alpha_{ij} < 1$ and for neutral or no interaction, $\alpha_{ij} \sim 1$. Table 1 shows the interaction between different cell types and the possible range of the resultant α values.

For the construction of the state bias matrix ($\bar{\Omega}$), numerical values for each α_{ij} were estimated as a first iteration after which the first experimental run has been executed. Based on the results of the initial run, alterations are made to the experimental parameters, including the α values, before the next run. This iterative procedure is repeated until a reasonable model is produced from these numerical parameters.

Table 1

Relationship between intercellular interactions and α

I	j	Molecular structure		Intermolecular force	Strength	Force direction	Rank*	α_{ij}
		i	j					
1	1	Void	Void	-	-	-	3	~1
1	2	Void	Non polar	-	-	-	3	~1
1	3	Void	Polar	-	-	-	3	~1
1	4	Void	Ionic	-	-	-	3	~1
1	5	Void	Ionic	-	-	-	3	~1
2	1	Non polar	Void	-	-	-	3	~1
2	2	Non polar	Non polar	Van der Waals Forces	Below average	Attracting	4	≤1
2	3	Non polar	Polar	Dipole—induced dipole	Average	Attracting	5	<1
2	4	Non polar	Ionic	Immiscible, i.e. negligible interaction	Weak	Repelling	2	≥1
2	5	Non polar	Ionic	Immiscible, i.e. negligible interaction	Weak	Repelling	2	≥1
3	1	Polar	Void	-	-	-	3	~1
3	2	Polar	Non polar	Dipole—induced dipole	Average	Attracting	5	<1
3	3	Polar	Polar	Dipole—dipole	Above average	Attracting	5	<1
3	4	Polar	Ionic	Ion-dipole	Strong	Attracting	5	<1
3	5	Polar	Ionic	Ion-dipole	Strong	Attracting	5	<1
4	1	Ionic	Void	-	-	-	3	~1
4	2	Ionic	Non polar	Immiscible, i.e. negligible interaction	Weak	Repelling	2	≥1
4	3	Ionic	Polar	Ion-dipole	Strong	Attracting	5	<1
4	4	Ionic	Ionic	Ionic	Strongest	Repelling	1	>>1
4	5	Ionic	Ionic	Ionic	Strongest	Attracting	6	~0
5	1	Ionic	Void	-	-	-	3	~1
5	2	Ionic	Non polar	Immiscible, i.e. negligible interaction	Weak	Repelling	2	≥1
5	3	Ionic	Polar	Ion-dipole	Strong	Attracting	5	<1
5	4	Ionic	Ionic	Ionic	Strongest	Attracting	6	~0
5	5	Ionic	Ionic	Ionic	Strongest	Repelling	1	>>1

*1 = largest α , 6 = smallest α

Simulation of fouling in membrane processes with cellular automata

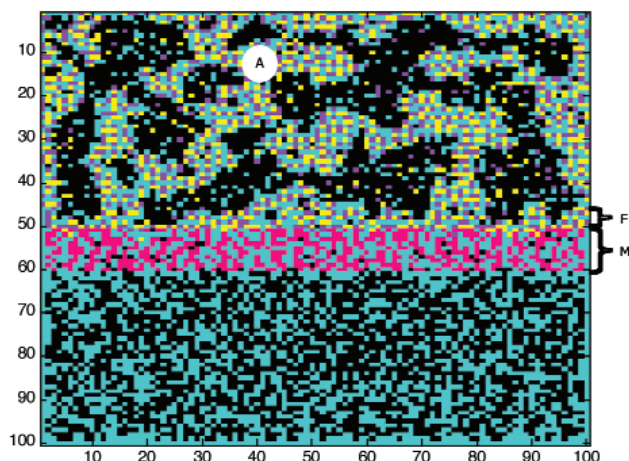


Figure 5—Visibility of fouling layers (F) on membrane surface (M) and salt agglomerates (A) after prolonged simulation with a cellular automata model

Discussion and conclusions

Figure 5 shows the typical state of the system after prolonged dynamic evolution during one of the trial runs. The build-up of a fouling layer that inhibits the permeability of the membrane can be clearly observed. It becomes evident that there is an optimal state bias that maximizes the degree of osmosis for a neutral directional bias. For the runs performed in this project, an average maximum of 57.4% displacement of water across the membrane could be obtained with the following state bias (Equation [6]):

$$\bar{\Omega}_y = \begin{Bmatrix} 1 \times 10^0 & 1 \times 10^3 & 1 \times 10^6 & 1 \times 10^{12} & 1 \times 10^{12} \\ 0 & 1 \times 10^3 & 1 \times 10^6 & 1 \times 10^{16} & 1 \times 10^{16} \\ 1 \times 10^6 & 1 \times 10^6 & 1 \times 10^3 & 1 \times 10^{-20} & 1 \times 10^{-20} \\ 0 \times 10^0 & 0 \times 10^0 & 0 \times 10^0 & 0 \times 10^0 & 0 \times 10^0 \\ 1 \times 10^{12} & 1 \times 10^{16} & 1 \times 10^1 & 0 \times 10^0 & 1 \times 10^{24} \end{Bmatrix} \quad [6]$$

The maximum degree of osmosis was achieved under low density conditions that resemble high temperature conditions. This agrees with the physical phenomenon that is observed when the temperature of a real-life osmotic system is increased. The temperature increase resembles the increase in kinetic energy owing to the heat energy transferred to the system. The kinetic energy in turn causes the water molecules to move faster, therefore an increased rate of osmosis is observed.

In addition to a low density and optimal interaction parameters, a high salt-to-water ratio increases the number of available spaces in the Moore neighbourhood surrounding the salt ions. This allows for an increased number of water molecules to interact with the ions in the form of a strong ion-dipole attractive force. Although it might seem that the high salt-to-water ratio as such is the answer to increased osmosis, the ultimate answer is less simple: The large number of ions tends to form clusters of water and ions, as shown in Figure 5, especially when two ions of opposite charge form a strong ionic bond. In the region of the upper compartment closest to the membrane, these clusters eventually prevent (physically obstruct) any further migration of water molecules towards the upper edge of the

compartment (away from the membrane). In order to prevent these blockages, the movement of the cells representing the ions can be restricted to prevent migration of the ions towards the membrane. This is not a realistic physical configuration in terms of geometry, but a compromise of the geometric accuracy for the modelled dynamic phenomena.

In spite of the above mentioned compromises, a simulator for membrane processes was successfully developed, based on the use of cellular automata. The software allows one to simulate potentially complex membrane processes by means of a few simple rules that encapsulate the physical phenomena occurring on a local level.

Although only the osmotic flow of a solution of salt through a membrane is considered here, the simulator can be extended to deal with a large variety of membrane processes and could provide valuable insights into potentially complex behaviour of these systems.

References

- AL-HALLAJ, S., ALASFOUR, F., PAREKH, S., AMIRUDDIN, S., SELMAN, J.R., and GHEZEL-AYAGH, H. Conceptual design of a novel hybrid fuel cell/desalination system. *Desalination*, vol. 164, no. 1, 2004. pp. 19–31.
- BENEŠ, P., ŠEBESTA, F., SEDLÁČEK, J., OBDRŽÁLEK, M., and ŠANDRIK, R. Particulate forms of radium and barium in uranium waste waters and receiving river waters. *Water Research*, vol. 17, no. 6, 1983. pp. 619–624.
- CUI, Z.F. AND WRIGHT, K.I.T. Flux enhancements with gas sparging in downwards crossflow ultrafiltration: Performance and mechanism. *Journal of Membrane Science*, vol. 90, 1994. pp. 183–189.
- DE LA TORRE, A.C. and MARTIN, H.O. A survey of cellular automata like the game of life. *Physica A: Statistical and Theoretical Physics*, vol. 240, no. 3–4, 1997. pp. 560–570.
- DEKKER, M. and BOOM, R. Improving membrane filtration processes, *Trends in Biotechnology*, vol. 13, 1995. pp. 129–131.
- FLETT, D.S. Solution purification. *Hydrometallurgy*, vol. 30, no. 1–3, 1992. pp. 327–344.
- KIER, L.B. and CHENG, C.-K. A cellular automata model of membrane permeability. *Journal of Theoretical Biology*, vol. 186, 1997. pp. 75–80.
- NENOV, V., LAZARIDIS, N.K., BLÖCHER, C., BONEV, B., and MATIS, K.A. Metal recovery from a copper mine effluent by a hybrid process. *Chemical Engineering and Processing* (In press). 2006.
- OLIVIER, J. and DE RAUTENBACH, C.J. The implementation of fog water collection systems in South Africa. *Atmospheric Research*, vol. 64, no. 1–4, 2002. pp. 227–238.
- SABBA, N. and AKRETICHE, D.-E. Selective leaching of a copper ore by an electromembrane process using ammonia solutions. *Minerals Engineering*, vol. 19, no. 2, 2006. pp. 123–129.
- SIPPER, M. *Machine Nature: The Coming Age of Bio-Inspired Computing*, McGraw-Hill, New York. 2002.
- VICHNIAC, G. Simulating physics with cellular automata. *Physica D*, vol. 10, 1984. pp. 96–115.
- VON NEUMANN, J. *Theory of Self-Reproducing Automata*. University of Illinois Press, Illinois, 1966. Edited and completed by A.W. Burks. 1966. ◆